THREE-DIMENSIONAL END EFFECTS IN IRON SEPTUM MAGNETS

J.-F. Ostiguy and D.E. Johnson

Fermi National Accelerator Laboratory *, P.O. Box 500, Batavia, IL 60510

Abstract

Among the technical difficulties encountered in designing an iron septum magnet, controlling the field quality at the longitudinal extremities of the field-free region is one of the most challenging. Without proper termination, flux jumping between the edge of the field-free region and the opposite pole piece results in a strong dipole kick and undesirable levels of higher order harmonics. The deleterious effects of the fringe field can be mitigated by reducing and channeling the leakage flux. We present 3D calculations and measurements performed on various end configurations for the Fermilab Main Injector iron septum magnets R&D program.

INTRODUCTION

In principle, an iron septum magnet, commonly referred to as a "Lambertson" is a simple device: a specially shaped hole is carved into one of the two pole pieces of a conventional dipole. Because of the high permeability of the iron, the flux circulates around the hole, establishing a so-called field-free region where the beam can drift freely. When a pulsed kicker is fired downstream of the septum magnet, the beam moves from the field-free region into the bending region where it is deflected and subsequently extracted into a beamline. The exact shape of the field-free region depends on many factors. For high-energy beams, the septum thickness is determined by the available kicker strength and is typically on the order of a few mm. The induction in the bending region is limited to 1.1-1.2 T since above that level, the septum region quickly saturates and the flux begins to penetrate into the field free-region. Using standard 2-D codes, it has become a relatively straightforward matter to design the cross section of an iron septum magnet. The field magnitude in the body of the magnet can easily be kept below a few Gauss; as a result, the bulk of the deleterious effect on the beam is due to the fringing flux at the longitudinal extremities of the magnet.

The end region must be analyzed as a fully three-dimensional problem; furthermore, saturation effects cannot always be neglected. Only five years ago, a typical run of a 3D finite-element code was limited to approximately 20000 nodes. The availability of faster processors and perhaps more importantly, of large amounts of physical memory has resulted in an order of magnitude increase in that number. Runs involving in excess of 10^5 nodes are now considered routine. Although 10^5 is a large number, one must keep in mind that linear resolution scales like the cube root of N. As a result, the mesh must be judiciously graded in order to obtain reliable results; this is an iterative process which tends to be time-consuming. Although 3D calculations are very useful for the magnet designer, they must be validated with measurements.

STRAIGHT END

As a starting point, it is instructive to understand and quantify what happens when no special precautions are taken to control the fringing flux. Consider the simple straight termination illustrated schematically in Figure 1. A plot of the vertical field along a line located 2.5 cm above the septum is shown in Figure 2. Note the sign inversion near the edge ($z = 0$), which is caused by the fact that some flux lines terminate inside the field-free region. Figure 2 and all the other results in this paper were obtained for a prototype of the magnet described in reference [1]. The coil is a symmetric saddle, the bending region is approximately 2 in × 14 in, and the bending field at full excitation is approximately 1.2 T (corresponding to 12×2000 A-turn/pole). The septum is approximately 5 mm thick. The agreement between measurement and calculation is excellent, despite the fact that the geometry was modeled rather crudely. For each extremity, the net dipole kick experienced by a particle traveling 2.5 cm above the septum would be 0.032 T-m. For the sake of comparison, at the same excitation, the field within the body of of the magnet is on the order of 8 Gauss. For a 3 m magnet, this represents a total body contribution of 0.0024 T-m, more than an order of magnitude smaller.
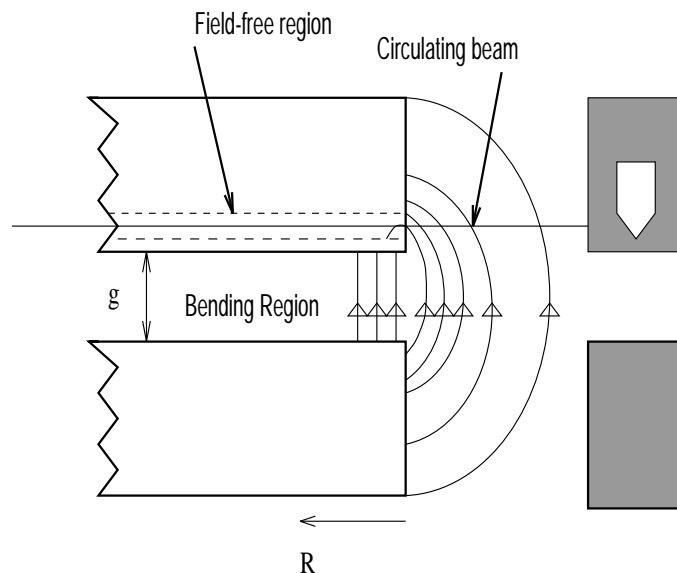

Figure 1. Longitudinal and transverse views of an iron septum magnet. The coils have been omitted to simplify the diagram. The circulating beam is shielded except in the end region where it traverses the fringe field. Some flux lines terminate inside the field free region, causing an inversion of the transverse field along the path of the beam.

EXTENDED END

To reduce the transverse field integral, the most obvious strategy consists in extending the pole containing the field-free region with respect to the other one. This method is effective, but only to a point. The relevant scaling here is the gap g; to reduce the integral by a factor n, the recess distance R (as shown in Fig. 1) must be on the order of $(n - 1)g$. Extraction regions are often quite busy from a lattice point of view; as a result space is tightly constrained, and it is not possible to increase the overall
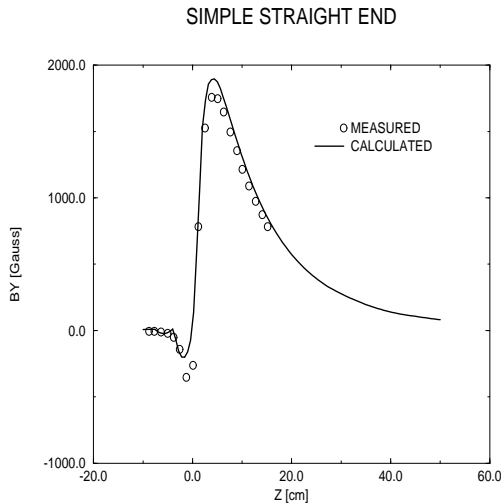
SIMPLE STRAIGHT END

Figure 2. Field of a simple straight end, along a line 2.5 cm above the septum wall. The agreement between measurement and 3D calculation is excellent.
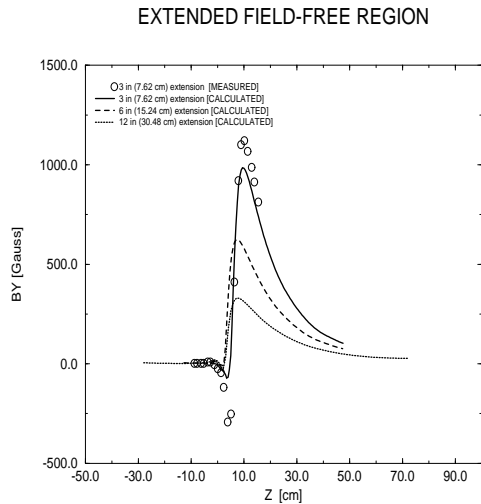
EXTENDED FIELD-FREE REGION

Figure 3. Fringe field of magnets with extended end region, along a line 2.5 cm above the septum wall. The dots corresponds to a measurement performed with $R = 7.62$ cm

length of the magnet much beyond what is required to provide sufficient deflection to extract the beam. Unequal pole lengths also degrade the field quality in the bending region; although not as critical, this degradation eventually becomes significant. A plot of the field for three different distances between the upper and lower cores is presented in Figure 3. As expected, the field integral scales inversely with with the average fringe path length $R + g$.

MIRROR PLATE

To minimize the overall length of the magnet while keeping the fringing field integral under control, one possible approach is to channel the leakage flux through a steel plate as illustrated in Figure 4. Instead of jumping to the opposite pole, the flux now travels longitudinally into the plate, is channelled around the field-free hole and returns into the opposite pole. Provided there is not too much saturation, the plate surface is approximately at constant magnetic potential and there should be no field beyond the outer edge of the plate. In the region between

the end of the field-free region and the plate, the flux has a transverse component, but the integrated effect cancels out due to symmetry. This explains why such a plate is sometimes referred to as a "mirror plate". Figure 5 is a plot of the measured and calculated field for the configuration illustrated in Figure 4. At low excitation, the plate has high permeability and the fringe field is completely quenched. At maximum excitation, the plate saturates considerably; the result is a drop in magnetic potential along the plate surface, hence the re-appearance of a long slowly decaying tail. To improve the situation, one needs to reduce the magnitude of the induction in the plate either by increasing the distance between the plate and the edge of the field-free region or by increasing the thickness of the plate. An important observation is that the magnetic potential drop in the plate is seriously affected by the width of the bending region aperture sides. This is illustrated in Figure 6 and 7. Note the dramatic increase in the field integral when this width is reduced to 2.5 cm.

CONCLUSION

We have demonstrated that 3D calculations of the fringe field at the extremities of an iron septum magnet are reliable. Such calculations have made it possible to understand and quantify the importance of saturation effects in a mirror plate.

ACKNOWLEDGMENTS

References

[1] D.E. Johnson et al., "Design of The Fermilab Main Injector Lambertson", These proceedings.
[2] M. Harrison and F.N. Rad, "Symmetric and Non-Symmetric Lambertson Magnets", Nucl. Inst. Meth. 227, (1984) 401-410
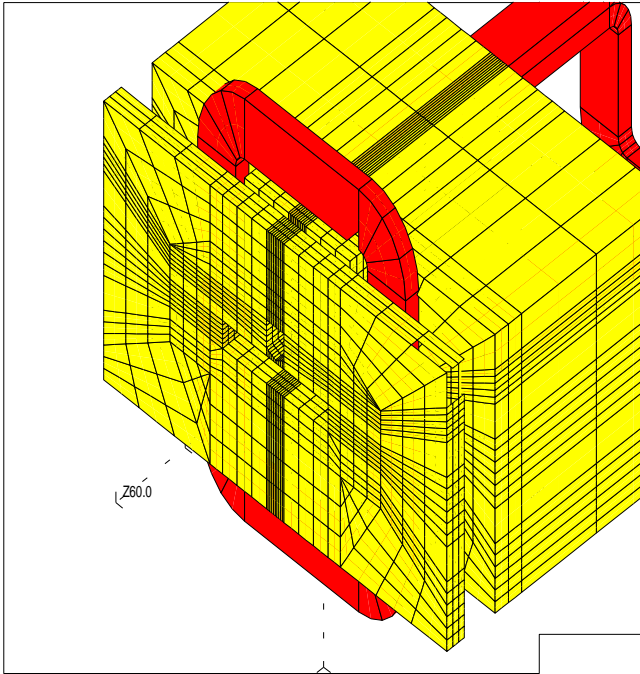
Figure 4. Mirror plate configuration. The field free-region has been extended 7.62 cm longitudinally. The plate is 2.54 cm thick and separated by 1.27 cm from the edge of the field-free region.
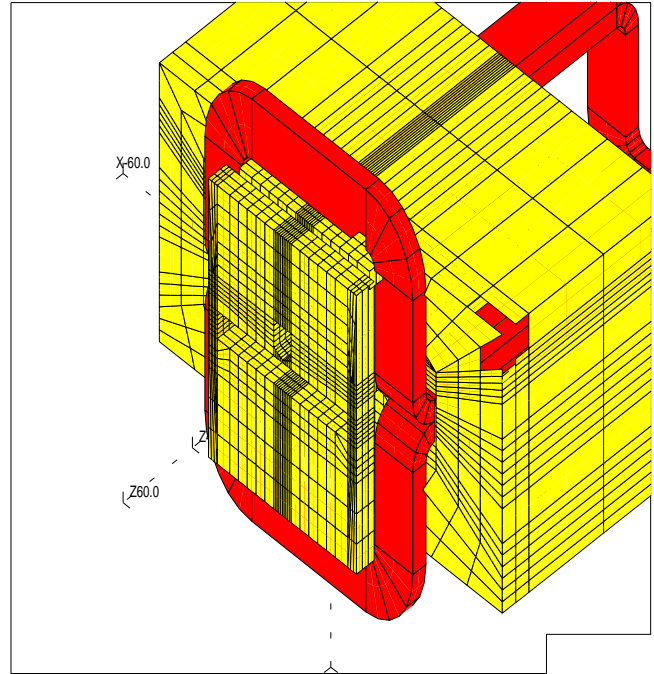

Figure 6. Mirror plate configuration. The geometry is the same as in Figure 4, but the plate width has been reduced. The sides of the bending region aperture are 2.54 cm wide.
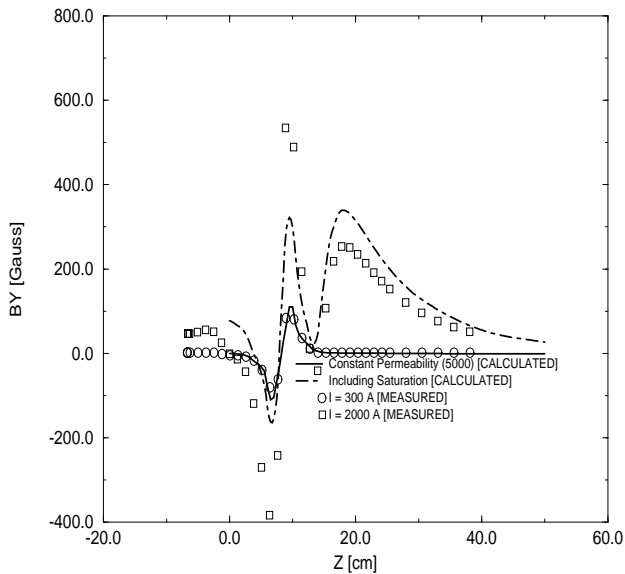

Figure 5. Calculated and measured fields for the configuration shown in Figure 4. The plot labeled "constant permeability" corresponds to $I = 300$ A. The field are plotted along a line located 2.54 cm above the septum wall.
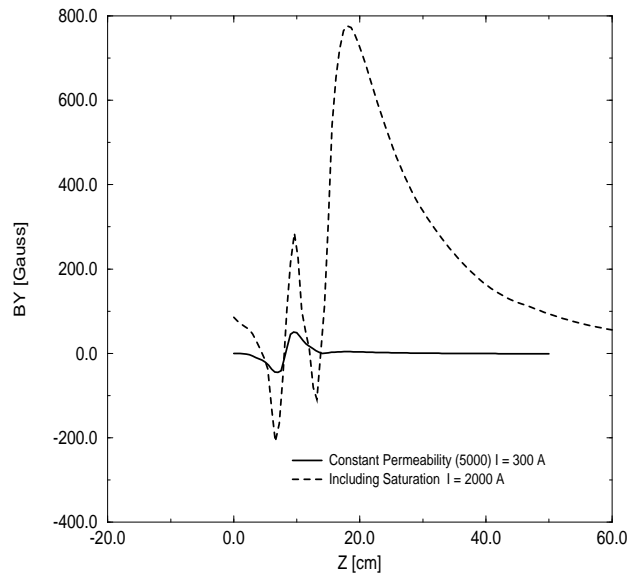

Figure 7. Calculated field for the configuration shown in Figure 6. The plot labeled "constant permeability" corresponds to $I = 300$ A. Note the increase in the size of the tail compared with Figure 5.